The phase transition sequence in the relaxor ferroelectric PZN–8% PT

2008 J. Phys.: Condens. Matter 20 165208

(http://iopscience.iop.org/0953-8984/20/16/165208)

J. Phys.: Condens. Matter **20** (2008) 165208 (8pp) doi:10.1088/0953-8984/20/16/165208

The phase transition sequence in the relaxor ferroelectric PZN–8% PT

E H Kisi and J S Forrester

School of Engineering, The University of Newcastle, NSW 2308, Australia

E-mail: Erich.Kisi@newcastle.edu.au and jenny.forrester@newcastle.edu.au

Received 18 January 2008, in final form 28 February 2008
Published 31 March 2008
Online at stacks.iop.org/JPhysCM/20/165208

Abstract

Crystal structures and phase transitions in the giant piezoelectric effect material lead zinc niobate–8% lead titanate (PZN–8% PT) between 4.2 and 455 K have been determined using very high resolution powder neutron diffraction. The structure at 4.2 K is monoclinic (Cm). On heating, the monoclinic phase transforms first into tetragonal ($P4mm$) and then cubic ($Pm3m$) structures via first-order transitions with wide two-phase regions.

1. Introduction

Single crystal relaxor ferroelectric materials in the $PbZn_{1/3}Nb_{2/3}O_3$–$PbTiO_3$ (PZN–PT) system, in particular those at the morphotropic phase boundary (MPB) with compositions PZN–8% PT and PZN–9% PT, have attracted considerable recent attention due to their excellent piezoelectric properties (e.g. piezoelectric coefficient d_{33}–2500 pC N^{-1}, piezoelectric strain 1.7%) [1, 2]. There has been much controversy in the literature over the mechanism underlying these properties, which are the highest recorded of any known material.

Several features of PZN–PT materials are at the root of the controversy. First, they have perovskite structures only marginally distorted from cubic. Their pseudo-cubic symmetry has made it difficult to ascertain the true symmetry as a function of temperature, composition, applied electric field and mechanical load. To the PZN side of the original PZN–PT phase diagram [1], the symmetry is shown as rhombohedral ($R3m$) and on the PT side, it is shown as tetragonal ($P4mm$), in common with the widely utilized $PbZr_xTi_{1-x}O_3$ (PZT). These two phases are separated by an MPB in which the symmetry has recently been described in various monoclinic or orthorhombic space groups. Second, unlike other ferroelectric materials, the maximum piezoelectric response and the spontaneous polarization are not co-linear. The large electromechanical coupling and piezoelectric strain occurs in the [001] direction (all directions are referred to the parent cubic phase) whereas the spontaneous polarization is along [111]. Third, the crystals contain microscopic ferroelectric domains [3, 4] which are affected by strain and interfere with single crystal structure investigations. Fourth, being relaxor ferroelectrics, the materials contain polar nano-domains most likely associated with the occupation of the B cation site by Nb, Zn and Ti in different ratios [5, 6].

Reviews of the proposed mechanisms have been undertaken by Noheda and Cox [7] and Davis *et al* [8], and here we summarize the prominent ones. An early mechanism for the giant piezoelectric response, and one that remains popular, is that PZN–PT has a large elastic compliance (s_{33}) which allows greater mechanical deformation along the principal axes per unit of applied electric field [1, 9, 10]. Ogawa *et al* [9] measured the elastic compliances in the rhombohedral and tetragonal regions in PZN–9% PT, and concluded that the $R3m$ phase was much more 'mechanically soft' than the $P4mm$ phase. These high elastic compliances are likely to have a significant influence on the other proposed mechanisms discussed below.

A second hypothesis is that the enhanced piezoelectric response is the result of electric field induced phase transitions. The bulk of this work originates from *in situ* x-ray and neutron diffraction studies of PZN–8% PT at various applied electric fields or after electric poling. Originally, an E-field induced phase transition from rhombohedral ($R3m$) to tetragonal ($P4mm$) was proposed [2, 11, 12]. In recent years, many lower symmetry structures have been proposed in the region of the MPB in PZN–PT and the archetypal MPB in PZT as discussed below.

A theoretical framework for comprehending the diversity of phases in this system is the polarization rotation mechanism proposed by Fu and Cohen [13]. In this view, the polarization vector is able to rotate between the spontaneous polarization in the rhombohedral phase [111], and the spontaneous polarization in the tetragonal phase [001], under an electric field applied along [001]. This theory and its exploration by expanding a Landau–Devonshire model to 12th order [14]

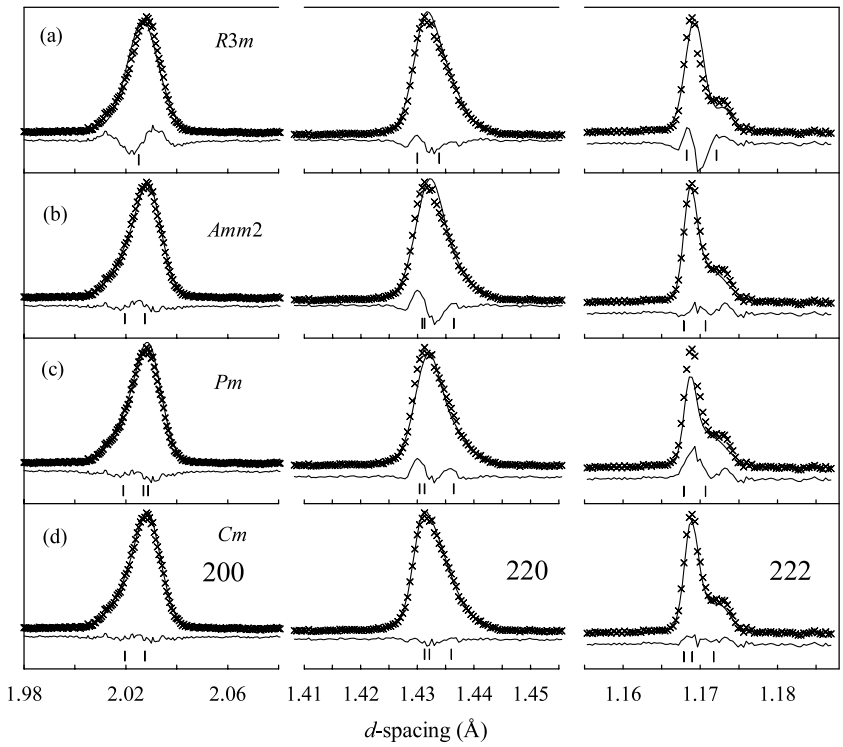

Figure 1. Rietveld fits to the diagnostic 200, 220 and 222 diffraction peaks at 4 K illustrating the agreement with structure models in (a) *R*3*m*, (b) *Amm*2, (c) *Pm* and (d) *Cm*.

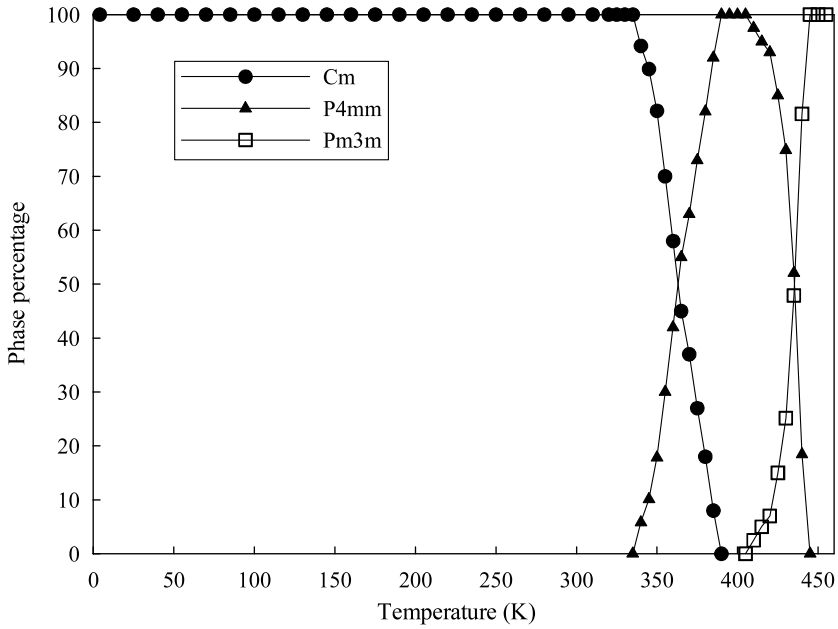

Figure 2. Phase percentages in PZN–8% PT as a function of temperature.

predicted various metastable or electric field induced phases at the MPB. These include a monoclinic phase in *Cm* (known as M_A) and related monoclinic phases (M_B and M_C) in *Pm* and *Cc* as well as an orthorhombic phase in *Amm*2. Each of the phases has been reported to occur experimentally in PZN–PT or the related material PMN-PT ($PbMg_{1/3}Nb_{2/3}O_3$–$PbTiO_3$) under various conditions. In PZT, the monoclinic phase in *Cm* rather than the traditional *R*3*m* + *P*4*mm* coexistence at the MPB in PZT was first observed by Noheda *et al* [15] and a new phase diagram was proposed [16]. Other work on PZT and PMN-PT has produced many observations and interpretations including but not restricted to; *R*3*m* + *Amm*2 [17], *R*3*c* + *Cm* [18], *Pm* [19, 20], *Cm* + *Cc* [21], and *Cc* [22]. In the PZN–PT system of interest here, the

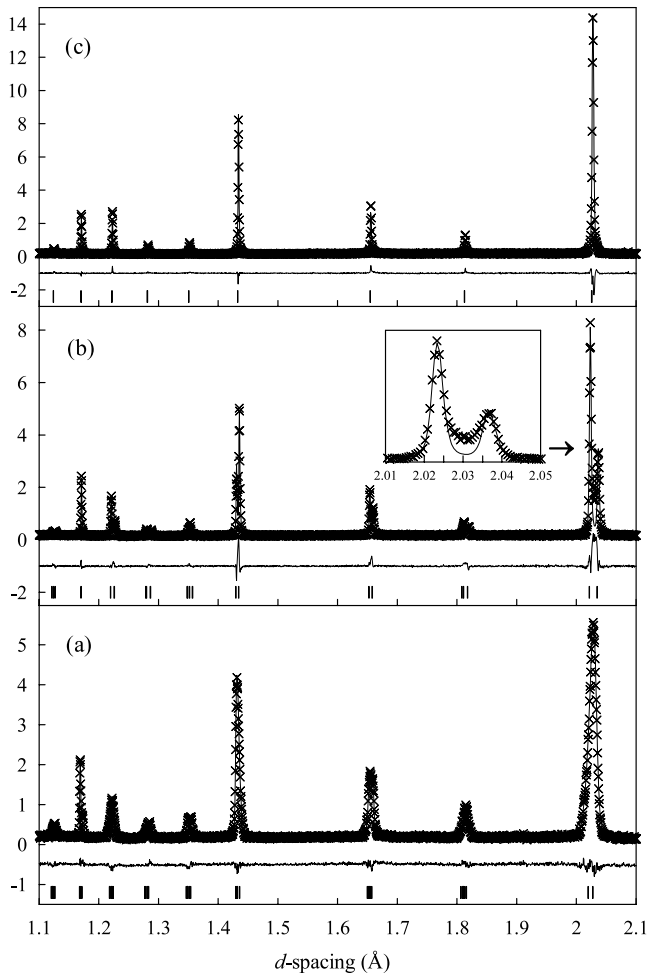

Figure 3. Rietveld refinement plots for (a) the monoclinic phase in *Cm* at 4 K, (b) the tetragonal phase in *P*4*mm* at 395 K and (c) the cubic phase in *Pm*3*m* at 455 K. For greater clarity, only the region between 1.1 and 2.1 Å is shown. Residual misfitting in (b) is due to domain wall scattering (inset).

MPB phase has been reported to be orthorhombic [17] or monoclinic in *Pm* [20]. Recent work by Davis *et al* [8] has concluded that there is an electric field induced distortion between rhombohedral–orthorhombic–tetragonal symmetries and argued that this polarization rotation is undoubtedly responsible for the giant piezoelectric response. The question of whether these are true phases or just distortions of the rhombohedral parent phase has been raised in [10], where it was demonstrated that ferroelectric (or elastic) distortion of a rhombohedral material in space group *R*3*m* along [001] results (temporarily) in monoclinic symmetry in space group *Cm*. Davis *et al* [8] conclude that this distinction does not affect the attribution of the large piezoelectric response to polarization rotation.

We have embarked on a programme of work to carefully re-examine the crystal structures and structural phase transitions in PZN–PT using very high resolution neutron diffraction. In our previous work on PZN the ground state symmetry *R*3*m* was found to convert directly to the cubic parent phase above the Curie temperature [23, 24]. PZN–4.5% PT single crystals were shown to be rhombohedral also in *R*3*m*, a structure which persists to approximately 390 K where there is a transition to *P*4*mm* [25]. A similar conclusion was reached using coarse powders, however a single phase tetragonal region was not found [26]. The motivation for this work is to determine as a function of temperature, the baseline structures and structural phase transitions at the composition showing the maximum piezoelectric effect (PZN–8% PT). This paper reports the results of a very high resolution neutron powder diffraction study of PZN–8% PT over the temperature range 4.2–455 K.

2. Experimental details

Single crystals of the composition $PbZn_{1/3}Nb_{2/3}O_3$–8%$PbTiO_3$ were grown in a PbO flux following the method of Mulvihill *et al* [27]. Crystals of various sizes ranging from 0.5–15 mm were extracted by dissolving the flux in a hot HNO_3 solution. To utilize the extreme resolution of the diffractometer to its greatest advantage, approximately 2 cm^3 of crystals were prepared by light crushing and passing through a 143 μm sieve. This allowed a compromise between good powder averaging without causing excessive particle size broadening or lattice strains.

Neutron powder diffraction patterns were recorded on the HRPD diffractometer at the ISIS facility, Rutherford Appleton Laboratory, UK. The instrument has a resolution of $\Delta d/d = 4 \times 10^{-4}$ in the absence of sample induced broadening. The crystals were loaded into a thin walled aluminium can within a liquid helium cryostat. Neutron diffraction patterns were recorded between 4.2 and 455 K, and from 30 000 to 120 000 μs whilst pausing at constant temperature for 20 min including 2 min for temperature equilibration.

Data from the high resolution backscattering bank were used in crystal structure refinements in the Rietveld analysis program GSAS [28]. Refinements usually included lattice parameters, atom coordinates, isotropic thermal parameters (Pb, Zn/Nb), anisotropic thermal parameters (O), scale, and 8 polynomial background parameters. The anisotropic peak broadening model of Stephens [29] was necessary to compensate for anisotropic peak broadening due to inter-domain strains.

There was an added complication in some of the refinements associated with domain wall scattering from the tetragonal phase. This phenomenon, where the observed intensity does not fall to the background but instead forms a plateau has been observed between twin-related peaks of ferroelectric materials and has been discussed in detail by Darlington and Cernik [30], Taylor and Swainson [31], and Valot *et al* [32]. This is difficult to model in Rietveld refinements, as the peak shape parameters are inclined to refine unphysical values in an attempt to account for this scattering. To counteract this effect, it was necessary to constrain some parameters in the two-phase regions. Specifically, lattice parameters were refined in all cases, however in the temperature ranges 340–385 K and 410–440 K parameters such as the phase fractions, histogram scale factors and anisotropic peak shape parameters, were altered manually by a lengthy trial and error process rather than the usual least squares procedure.

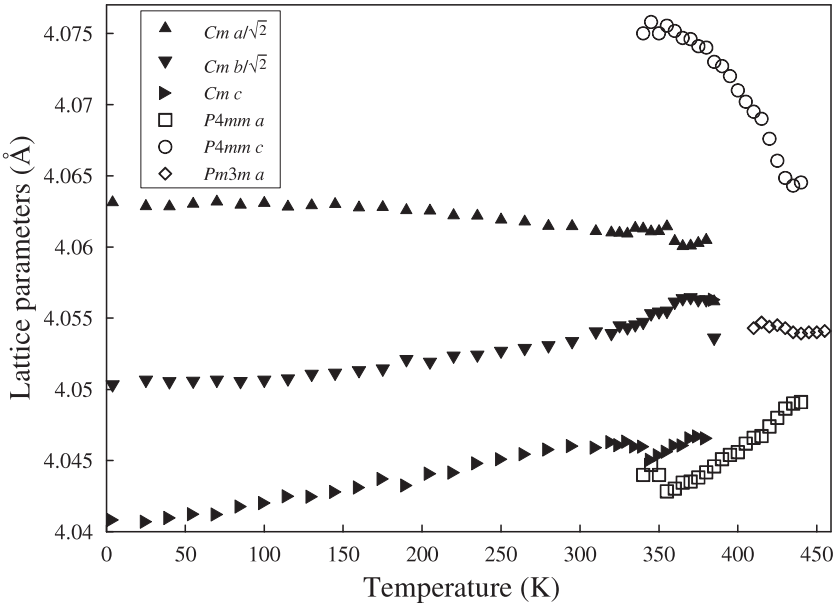

Figure 4. Refined lattice parameters for the PZN–8% PT structures as a function of temperature.

3. Results and discussion

3.1. The ground state

Details of the crystal structure solution process, refined atom coordinates and structure diagram at 4 K have been published elsewhere [33]. In brief, pseudo-symmetry and sample induced peak broadening prevent the application of traditional means of structure solution. Instead Rietveld refinements were trialled with equal effort in all the space groups and combinations which have been suggested in the literature for the morphotropic boundary in the PZN–PT system and which do not involve coupled octahedral rotations. Selected diffraction peaks from each of the refinements at 4 K are shown in figure 1. The peaks selected (200, 220 and 222) represent the three principal directions in the Devonshire expansion for the free energy of a ferroelectric.

Since the ground state of PZN and PZN–4.5% PT have been confirmed to be rhombohedral in $R3m$ [23–26], this was the logical starting point. On the scale of an entire diffraction pattern this model fits the data reasonably well however, as can be seen in figure 1(a), there are serious errors which cannot be rectified with the structural and line broadening parameters available. In particular, the observed 200 peak is split and the calculated peak is out of position. Likewise, the calculated 222 peak is out of position. Attempts to fit the data as a two-phase mixture of rhombohedral and tetragonal, or rhombohedral and orthorhombic phases were not successful [33]. Single phase fits to the orthorhombic ($Amm2$) and monoclinic (Pm, Cm) structures are shown in figures 1(b)–(d). Lengthy attempts to improve the fit in Pm and $Amm2$ both by least squares refinements or manual intervention failed. The structure in Cm clearly fits the data best and is the correct structure for the ground state of PZN–8% PT.

Table 1. Phase fields in PZN–8% PT.

Temperature range (K)	Phases present	Space groups
$4 \Rightarrow 335$	M	Cm
$340 \Rightarrow 385$	M + T	$Cm + P4mm$
$390 \Rightarrow 405$	T	$P4mm$
$410 \Rightarrow 440$	T + C	$P4mm + Pm3m$
$445 \Rightarrow 455$	C	$Pm3m$

3.2. Phase transitions

Although the greater pseudo-symmetry at 295 K makes the distinction between Pm and Cm less definite, a similar series of trial refinements as described above was conducted at that temperature with the same conclusion. Refinements were then undertaken using all data recorded at temperatures from 4 to 455 K. The monoclinic structure was found to be the only phase present in the range 4–335 K. Above that, a broad two-phase region containing the Cm phase and the tetragonal phase in $P4mm$ was observed. The tetragonal structure, which could not be observed as a single phase at 4.5% PT [26], now occupies a band at least 15 K wide. Above 410 K, is a further small two-phase region showing coexistence of the $P4mm$ phase and the parent cubic phase in $Pm3m$. A summary of the structures in the temperature range 4–455 K from the Rietveld refinements is shown in table 1 and the phase proportions are plotted in figure 2. As noted above, due to instabilities in some two-phase refinements where only small amounts of one phase was present, some parameters were *manually* refined by a trial and error process rather than the usual full-matrix least squares procedure. Due to pseudo-symmetry and strain induced reflection broadening, we believe that the parameters obtained in this way are more reliable.

An extended portion of the Rietveld refinements for each of the single phases is shown in figure 3. The fit to the monoclinic phase in Cm (figure 3(a)) confirms the correctness

of that structure. The fit to the tetragonal phase (figure 3(b)) is also good except that the tetragonal phase has a significant amount of domain wall scattering in between the twin-related peaks such as 002/200. This kind of scattering has been remarked upon several times (e.g. [30]) and phenomenological models developed [31, 32, 34]. Based purely on the non-Bragg reflection area as a ratio to the total diffraction above background for this pair of reflections, we can estimate the strained region around domain walls to represent ∼15% of this material. The fit to the cubic phase (figure 3(c)) is good though unremarkable.

Figure 4 shows the pseudo-cubic lattice parameters for the three phases over the entire temperature range investigated[1]. Several features are apparent. With increasing temperature in the *Cm* region, there is a fairly smooth decrease in a with a corresponding and larger increase in b and c. It is of interest to extrapolate the region above 200 K (free from low temperature saturation effects) and below ∼320 K (free from curvature due to impending transitions) to high temperature. In the extrapolation, $a_m/\sqrt{2}$ and $b_m/\sqrt{2}$ converge at around 650 K to form a pseudo-tetragonal metric. Convergence with c_m to give a cubic metric is much higher at around 900 K. Instead, the tetragonal phase intrudes at a much lower temperature. The transition to the tetragonal phase is preceded by some downward curvature of c_m and upward curvature of $b_m/\sqrt{2}$ however there is little doubt that the transition is first order from both the observed spontaneous strains and the broad two-phase region. The lattice parameters of the tetragonal phase indicate initial spontaneous strains $\varepsilon_{11} \approx 0.0025$ and $\varepsilon_{33} \approx 0.0055$ which are smaller than those reported for $BaTiO_3$ [35]. Curiously, the usual thermodynamic requirement that non-interacting phases in a two-phase region have constant lattice parameters is violated in both the monoclinic *and* tetragonal phases although the trends at the extreme ends of the two-phase regions (e.g. the tetragonal phase at 340, 345, 350 and 440 K) are not precise due to the small amount of one of the phases. The effect is illustrated in figure 5 to not be an artefact of the Rietveld fitting but rather a genuine trend in the peak positions. A plausible rationale for this observation is that the two phases form coherent boundaries within the microstructure and the associated misfit strains have the same form as the thermodynamic strains. The tetragonal parameters trend towards cubic at an extrapolated temperature of 465 K although the cubic phase appears via a first order transition much lower than that. The tetragonal lattice parameters found here and those of our previous study on PZN–4.5% PT [26] behave similarly however, unlike here, in PZN–4.5% PT no single phase tetragonal region was found. PZN–8% PT becomes cubic at 445 K.

The temperature evolution of the refined monoclinic β angle, shown as the spontaneous shear strain (ε_{13}) in figure 6, appears continuous in stark contrast with the lattice dimensions in figure 4. Unlike the lattice dimensions, extrapolation of the monoclinic distortion ($\beta - 90°$) indicates a monoclinic → orthogonal transition at approximately 374 K. The extrapolation is assisted by least squares fitting to an equation of the form:

$$\beta - 90 = C\left[T_C\left(\frac{1}{\tanh\left(T_S/T_C\right)}\right) - \left(\frac{1}{\tanh\left(T_S/T\right)}\right)\right]^{\frac{1}{2}} \quad (1)$$

with constant $C = 0.010\,02$, critical temperature $T_C = 374$ K and saturation temperature $T_S = 177$ K. The fit is quite reasonable however, for these space groups, equation (1) describes a tri-critical transition as discussed previously for PZN [21], whereas the transition here is clearly first order. Nonetheless, the fit does give some general indicators concerning the transition e.g. the critical temperature determined here, 374 K, is slightly lower than that for PZN

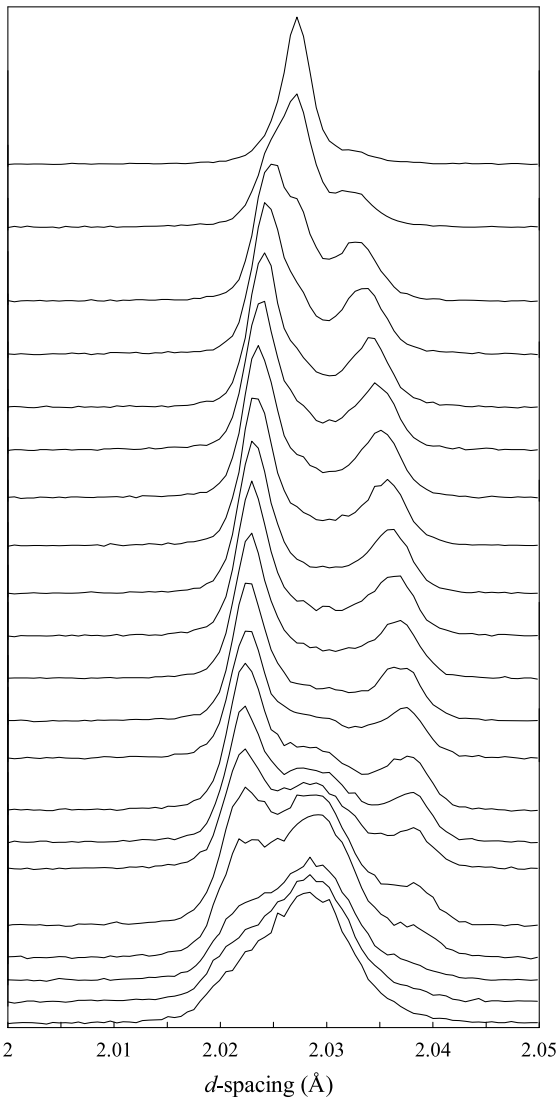

Figure 5. Tetragonal splitting of the 200 reflection as a function of temperature illustrating that the spontaneous strain evolves over the whole range of temperature irrespective of two-phase coexistence. At the bottom of the figure is the first appearance of the T-phase at 340 K where the majority of the material is M-phase. The series shows the progression through the pure T-phase and into the T + C region. Beyond the topmost pattern shown, the material is wholly cubic.

[1] In the single phase monoclinic region of figure 4, the estimated standard deviations for the lattice parameters a, b and c are 0.0002 Å, 0.0003 Å and 0.0003 Å respectively. For a and c in the tetragonal region, they are 0.000 03 Å and 0.000 05 Å respectively and for the cubic parameter a, it is 0.000 06 Å. These values increase by up to a factor 3 in the two-phase regions.

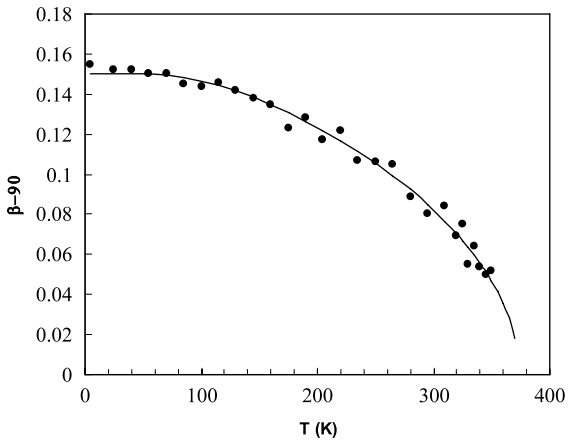

Figure 6. Illustrating changes to the spontaneous shear strain in the monoclinic phase with increasing temperature and a fit to equation (1). The standard deviations in these angles, estimated during Rietveld refinement, are 0.003°.

(384 K) and considerably lower that for PZN-4.5% PT (407 K) determined in the same way.

Unit cell volumes estimated from the refined lattice parameters are shown in figure 7 for the single phase regions. Despite the transitions being very different in nature (M → T → C and R → C) the curve has all of the features noted in the analogous curve for PZN [24]. These include, on heating, a slight change of slope near 200 K above which the thermal expansion is very similar to that of the cubic phase, and a lattice contraction upon heating through the transition to cubic. Rather than the usual explanation due to the rotation of rigid structural units, this region of apparent negative thermal expansion in PZN is attributed to a geometrically imposed volume-dilation on cooling due to the onset of the polarized state and its effect on the packing efficiency, particularly of the B cations. Other ferroelectric phases such as $BaTiO_3$ show similar effects when examined closely (e.g. figure 2 of [30]).

3.3. Line broadening

Unlike PZN which showed only minor anisotropic peak broadening, very large anisotropic peak broadening parameters resulted from the refinements for PZN–8% PT as illustrated in figure 8. The origin of the broadening has not been absolutely determined although it is most likely of microstructural origin as follows. Being ferroelectric, on cooling each cubic crystal divides into tetragonal domains in such a way as to minimize the macroscopic strain. The strong domain wall scattering observed from the tetragonal phase shows that a considerable amount of the material is situated within the domain walls. The transition to the monoclinic structure on cooling involves further partitioning of each tetragonal domain into multiple monoclinic domains. In essence, there is little monoclinic crystal that is not part of one domain wall or another. As the temperature decreases, the lattice parameters deviate more from their cubic values and so the amount of broadening increases to accommodate the greater difference in the shape of adjoining domains. In figure 8 the reverse process is observed wherein the broadening decreases as the temperature increases. Coupled with these microstructural factors, there are undoubtedly some changes in the elastic constants as the phase transitions are approached.

In PZN, well resolved critical behaviour around the transition to cubic was apparent in the peak broadening parameter S_{400} [24]. Although the data scatter more widely here, critical behaviour surrounding the transition from monoclinic to tetragonal was observed in only one parameter, S_{220}, as shown in the inset to the figure. The peak in S_{220} is at 335 K, the upper limit of the single phase monoclinic region and is clearly associated with the phase transition. The

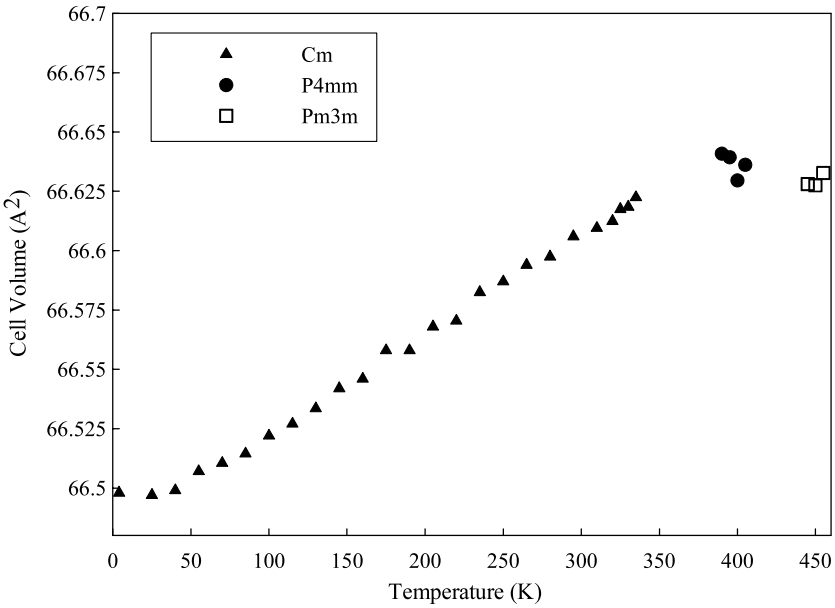

Figure 7. Unit cell volume of PZN–8% PT. Only single phase regions are shown. The estimated standard deviations are 0.005 $Å^3$, 0.001 $Å^3$ and 0.002 $Å^3$, respectively, for monoclinic, tetragonal and cubic single phases shown.

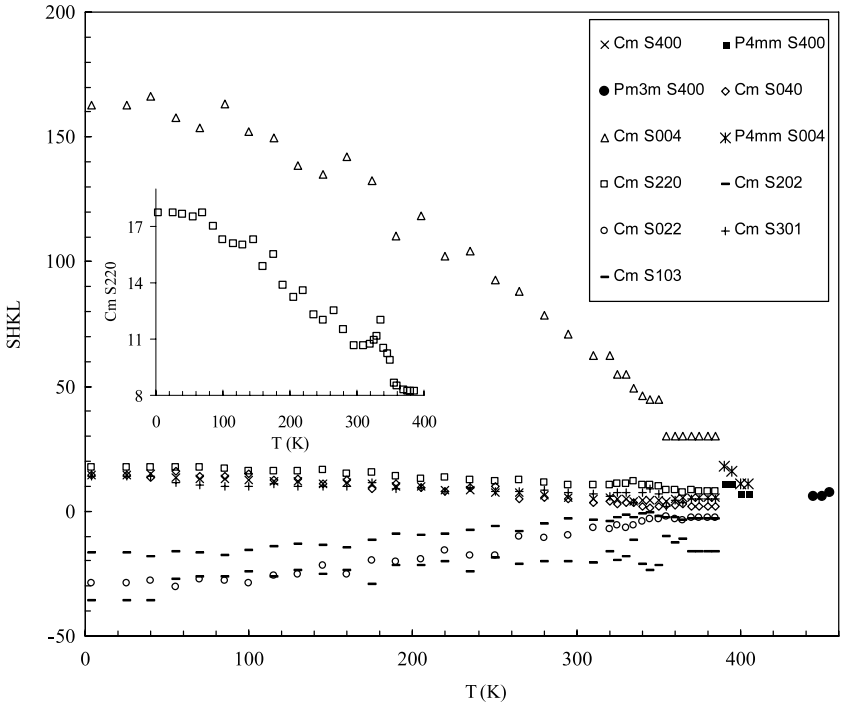

Figure 8. Anisotropic peak broadening parameters for the monoclinic phase refined using the model of Stephens (1999) in the program GSAS (1994). Parameters are also shown for the tetragonal and cubic single phase regions.

notation S_{220} refers to the monoclinic unit cell. This parameter is derived from S_{400} ($\equiv S_{004}$) if referred back to the pseudo-cubic unit cell and therefore the trend is exactly analogous to that observed for PZN. This effect is directed along the unit cell edges of both the parent cubic and the rhombohedral PZN structures—the direction in which the large piezoelectric effect is observed in PZN–PT and maximized in PZN–8% PT.

3.4. Origins of the giant piezoelectric effect in PZN–PT

This work has confirmed the existence of a pure monoclinic phase (*Cm*) at the morphotropic phase boundary in the PZN–PT system at 8% PT. It is of interest to consider the implications of this confirmation with respect to the theories of large piezoelectric response materials considered in the introduction (phase transition, polarization rotation or elastic softening). We ask the fundamental question *'does the observation of a monoclinic phase in and of itself explain the giant piezoelectric response?'* The answer to this is clearly *'no'* for the following reasons.

(i) PZN and PZN–4.5% PT show a large piezoelectric response in their own right and are clearly rhombohedral [23–26]. The observation, at these two compositions, of monoclinic symmetry upon the application of an electric field along [001] of the rhombohedral unit cell is entirely consistent with the expected piezoelectric distortion for any rhombohedral ferroelectric under these conditions [10] and does not constitute a phase transition.

(ii) The phase transition mechanisms are based purely upon a consideration of symmetry and *a priori* yield no information concerning the *magnitude* of the piezoelectric response. For example, it is widely accepted that at very high field, the material becomes tetragonal—and yet we find that the tetragonal phase has only a small spontaneous strain and associated spontaneous polarization. Further, the elastic constants of the tetragonal phase are reportedly far stiffer than the rhombohedral or monoclinic phases [9] indicating a smaller induced polarization per unit of applied field. Only detailed ion coordinates under applied electric field can allow tracking of both the magnitude and direction of the net (spontaneous + induced) polarization.

(iii) If polarization rotation alone can cause the large piezoelectric response, then there is an implicit assumption that the spontaneous polarization in the ground state (rhombohedral or monoclinic) phase is sufficiently large to account for the observed piezoelectric effect. In fact, a study of the spontaneous polarization in the rhombohedral phase of PZN has shown it to be small—being comparable to that in the rhombohedral phase of $BaTiO_3$ [24]. Indeed, the founding work of Fu and Cohen on polarization rotation [13] could only reproduce the observed piezoelectric enhancement if the material has 'a flat energy surface (i.e. soft force constants for ferroelectric displacements) near the rhombohedral phase' which is equivalent to the soft elastic constants postulate of Kuwata *et al* [1] and Ogawa *et al* [9].

The only mechanism consistent with all of the observations to date is that the particular combination of B-site ions lead to a large elastic softening along [001] which is then responsible not only for the observed piezoelectric behaviour but also the diverse structural behaviour.

4. Conclusions

This work has shown that the ground state of *un-poled* PZN–8% PT is monoclinic in space group *Cm*. The monoclinic phase persists as a single phase to above room temperature (335 K) and is therefore the phase on which most of the large piezoelectric response experimental studies have been conducted. Above 335 K there is a transition to a tetragonal phase ($P4mm$) followed by a transition to the cubic perovskite form ($Pm3m$). Based upon symmetry considerations alone, both of these transitions are allowed to be continuous. However, the monoclinic shear strain decays at an apparently tri-critical rate whereas the lattice parameters (hence deviatoric spontaneous strains) and two-phase coexistence indicate that both transitions are first order. Some weak critical behaviour was observed in the neutron diffraction peak broadening parameter providing evidence for elastic softening along [001] (referred to the parent cubic cell) in common with the rhombohedral phase of PZN [24]. This and an analysis of the evidence to date lead us to conclude that the existence of the monoclinic phase does not give a satisfactory explanation for the giant piezoelectric effect.

Acknowledgments

Many thanks for the assistance with data collection given by Kevin Knight of the ISIS facility, Rutherford Appleton Laboratory, UK. The work has been supported by the Australian Research Council grant DP0666166, the Australian Institute of Nuclear Science and Engineering, and the Access to Major Research Facilities Programme.

References

[1] Kuwata J, Uchino K and Nomura S 1981 *Ferroelectrics* **37** 579–82
[2] Park S-E and Shrout T R 1997 *J. Appl. Phys.* **82** 1804–11
[3] Fujishiro K, Vlokh R, Uesu Y, Yamada Y, Kiat J-M, Dkhil B and Yamashita Y 1998 *Japan. J. Appl. Phys.* **37** 5246–8
[4] Madeswaran S, Rajasekaran S V, Jayavel R, Ganesamoorthy S and Behr G 2005 *Mater. Sci. Eng.* B **120** 32–6
[5] Gehring P M, Park S-E and Shirane G 2001 *Phys. Rev.* B **63** 224109
[6] Welberry T R, Goossens D J and Gutmann M J 2006 *Phys. Rev.* B **74** 224108
[7] Noheda B and Cox D E 2006 *Phase Transit.* **79** 5–20
[8] Davis M, Damjanovic D and Setter N 2006 *Phys. Rev.* B **73** 014115
[9] Ogawa T, Yamauchi Y, Numamoto Y, Matsushita M and Tachi Y 2002 *Japan. J. Appl. Phys.* **41** L55–7
[10] Kisi E H, Piltz R O, Forrester J S and Howard C J 2003 *J. Phys.: Condens. Matter* **15** 3631–40
[11] Paik D-S, Park S-E, Wada S, Liu S-F and Shrout T R 1999 *J. Appl. Phys.* **85** 1080–3
[12] Durbin M K, Jacobs E W, Hicks J C and Park S-E 1999 *Appl. Phys. Lett.* **74** 2848–50
[13] Fu H and Cohen R E 2000 *Nature* **403** 281–3
[14] Vanderbilt D and Cohen M H 2001 *Phys. Rev.* B **63** 094108
[15] Noheda B, Cox D E, Shirane G, Gonzalo J A, Cross L E and Park S-E 1999 *Appl. Phys. Lett.* **74** 2059–61
[16] Noheda B, Gonzalo J A, Cross L E, Guo R, Park S-E, Cox D E and Shirane G 2000 *Phys. Rev.* B **61** 8687–95
[17] La-Orauttapong D, Noheda B, Ye Z-G, Gehring P M, Toulouse J, Cox D E and Shirane G 2002 *Phys. Rev.* B **65** 144101
[18] Frantti J, Ivanov S, Eriksson S, Rundolf H, Lantto V, Lappalainen J and Kakihana M 2002 *Phys. Rev.* B **66** 064108
[19] Singh A K and Pandey D 2003 *Phys. Rev.* B **67** 064102
[20] Noheda B, Cox D E, Shirane G, Gao J and Ye Z-G 2002 *Phys. Rev.* B **66** 054104
[21] Noheda B, Wu L and Zhu Y 2002 *Phys. Rev.* B **66** 060103
[22] Woodward D I, Knudsen J and Reaney I M 2005 *Phys. Rev.* B **72** 104110
[23] Kisi E H, Forrester J S and Knight K S 2006 *Acta Crystallogr.* C **C62** i46–8
[24] Forrester J S, Kisi E H, Knight K S and Howard C J 2006 *J. Phys.: Condens. Matter* **18** L233–40
[25] Forrester J S, Piltz R O, Kisi E H and McIntyre G J 2001 *J. Phys.: Condens. Matter* **13** L825–33
[26] Forrester J S, Kisi E H and Knight K S 2006 *Physica* B **385/386** 160–2
[27] Mulvihill M L, Park S-E, Risch G, Li Z, Uchino K and Shrout T R 1996 *Japan. J. Appl. Phys.* **35** 3984–90
[28] Larson A C and Von Dreele R B 2004 General structure analysis system (GSAS) *Los Alamos National Laboratory Report* LAUR 86-748
[29] Stephens P 1999 *J. Appl. Crystallogr.* **32** 281–9
[30] Darlington C N W and Cernik R J 1991 *J. Phys.: Condens. Matter* **3** 4555–67
[31] Taylor D R and Swainson I P 1998 *J. Phys.: Condens. Matter* **10** 10207–13
[32] Valot C M, Floquet N, Mesnier M T and Niepce J C 1996 *Mater. Sci. Forum* **228** 59–66
[33] Forrester J S and Kisi E H 2007 *Acta Crystallogr.* C **63** i115–8
[34] Taylor D R 2000 *Solid State Commun.* **116** 447–9
[35] Darlington C N, David W I F and Knight K S 1994 *Phase Transit.* **48** 217–36